

Product or sum: comparative tests of Voigt, and product or sum of Gaussian and Lorentzian functions in the fitting of synthetic Voigt-based X-ray photoelectron spectra

R. Hesse,* P. Streubel and R. Szargan

Wilhelm-Ostwald-Institute for Physical and Theoretical Chemistry, University of Leipzig, Linnéstr.2, D-04103 Leipzig, Germany

Received 7 July 2006; Revised 22 September 2006; Accepted 27 September 2006

A comparative study for the fitting of X-ray photoelectron spectra (XPS) using different model functions is presented. Synthetically generated test spectra using Gaussian/Lorentzian convolution and a real measured spectrum are fitted with the three commonly used models: product, sum and Gaussian/Lorentzian convolution functions. In these limited tests, it was found that the sum function is superior to the product function, particularly for low-noise spectra. Copyright © 2007 John Wiley & Sons, Ltd.

KEYWORDS: photoelectron spectroscopy; peak fit; Gaussian and Lorentzian functions; product function; sum function; Voigt profile

INTRODUCTION

Peak-fit programs for the modelling of X-ray photoelectron spectra (XPS) generally use a combination of a Lorentzian (or in case of asymmetric lines the Doniach–Sunjic function¹) and a Gaussian function.² The applied model depends on the program code of the employed software³ (Table 1). Available options give the operator the possibility to select a different model function in their analysis of the spectra. But recommendations for choosing the optimal model function for fitting XPS spectra are mostly not given.

The intensity distribution of photoelectron spectra may be modelled mathematically by a convolution of independent Lorentzian and Gaussian functions giving the so-called Voigt profile. In order to simplify the expensive convolution procedure, the product or, alternatively, the sum of the Lorentzian and Gaussian function designed with the same parameter set were proposed to approximate the Voigt profile of a real spectrum.

The question to be answered here is: what is the better alternative to the Voigt function, the product or the sum function? The significant difference in the product and Voigt profiles has already been demonstrated.⁴

In order to study this problem, four synthetic test spectra were generated with the software package MICROCAL ORIGIN. The result of their analysis using the sum-type, the product-type and the Voigt-model functions applying the program UNIFIT 2006⁵ are discussed and compared.

Finally, the three different methods were tested on a Cu 3p spectrum of a reference sample.

THEORETICAL BACKGROUND

Quantities for peak-fit evaluation and optimization

Generally, the analysis of XPS spectra is performed by comparing the experimentally recorded spectral intensity distribution with a theoretical model curve. The particular peak model parameters, e.g. peak position and intensity, are determined iteratively by a non-linear parameter estimation routine. The Marquardt–Levenberg algorithm⁶ has been chosen very often in order to minimize the reduced chi-square χ^{2*} (Eqn (1)).⁷ The final set of peak parameters, characterized by the parameter vector \vec{p} , are taken from the minimum of $\chi^{2*}(\vec{p})$, determined by the expression

$$\chi^{2*}(\vec{p}) = \frac{1}{N-P} \sum_{i=1}^N \frac{[M(i) - S(i, \vec{p})]^2}{M(i)} \quad (1)$$

with the measured spectrum $M(i)$ recorded at N energy values corresponding to channel i , the synthesized model curve $S(i, \vec{p})$ and P independent parameters of the model function. Another quantitative measure for discovering correlations in the residuals and thus problems with an inadequate model function or with incorrect working spectrometer components is the so-called *Abbe* criterion defined by⁷

$$Abbe = \frac{1}{2} \frac{\sum_{i=1}^{N-1} [R'(i+1) - R'(i)]^2}{\sum_{i=1}^N [R'(i)]^2} \quad (2)$$

*Correspondence to: R. Hesse, Wilhelm-Ostwald-Institute for Physical and Theoretical Chemistry, University of Leipzig, Linnéstr.2, D-04103 Leipzig, Germany.
E-mail: rhesse@uni-leipzig.de

Table 1. Examples of XPS data processing software and the available model functions

Software	Available model functions		
	Convolution	Product	Sum
UNIFIT for Windows, Version 2006 www.uni-leipzig.de/~unifit	X	X	–
CasaXPS www.casaxps.com	–	X	X
SpecsLab 1.8.2 www.specs.de/products/ESCA/software/vacos/specslab.htm	–	X	–
XPSPEAK 4.1 www.phy.cuhk.edu.hk/%7Esurface/XPSPEAK/	–	X	X
FitXPS2 ftp://boopic.ifa.au.dk/pub/fitxps/fitxps212.zip	X	–	–
wxEWA wxewa.sourceforge.net	X	–	X

with the residual function $R'(i) = S(i, \vec{p}) - M(i)$. The calculated value of the *Abbe* criterion may indicate three limiting cases:

- Abbe* → 0 systematically correlated residuals and therefore a bad choice of model function or erroneous working spectrometer components,
- Abbe* ≅ 1 statistically distributed residuals and thus random noise,
- Abbe* → 2 systematically anti-correlated residuals, also a reason to be suspicious.

It is strongly recommended that a plot of the normalized residuals $R(i)$ be included in the presentation of the measured data together with the optimized model curve $S(i, \vec{p})$ and individual components⁷

$$R(i) = \frac{S(i, \vec{p}) - M(i)}{\sqrt{M(i)}} \quad (3)$$

A statistically distributed $R(i)$ may already be a strong hint for a successful fit with the chosen fit conditions. But the accuracy of the fitted parameters can only be evaluated by calculating the standard deviation of the fit parameters.⁷

Modelling the peak shape

The energy (E) distribution curves in photoelectron spectroscopy may be characterized by spectral functions, which take into account all the possible excitation processes in the sample of interest. In the majority of cases, these spectral functions may be represented by a set of peaks, e.g. main line and satellites, each composed of multiplets, doublets or even single lines. The peak shapes are typically determined by a Lorentzian contribution due to the limited lifetime of the core hole state and a Gaussian broadening, mostly due to line shape of the exciting X rays from an X-ray monochromator, and electron scattering and detection in the spectrometer. Gaussian contributions may also be related to thermal excitation processes. Chemical, structural and electronic (by dopants) inhomogeneities in the surroundings of the emitting atoms often also contribute to the Gaussian broadening.

Both the Lorentzian function $L(E)$ (Fig. 1)

$$L(E) = \left\{ 1 + \left[\frac{(E - E_0)}{\beta} \right]^2 \right\}^{-1} \quad (4)$$

and the Gaussian function $G(E)$ (Fig. 1)

$$G(E) = \exp \left\{ -\ln 2 \left[\frac{(E - E_0)}{\beta} \right]^2 \right\} \quad (5)$$

are completely characterized by the peak parameters β , corresponding to 1/2 of the full width at half maximum ($FWHM = 2 \times \beta$), and the peak position E_0 .

Two frequently used approximations to describe XPS core-level lines are a product (Eqn (6), Fig. 2)^{2,8,9} and a sum (Eqn (7), Fig. 2)^{10–12} of Gaussian and Lorentzian functions of the same width. In order to include asymmetrical lines also, the peak-width parameter β may be substituted with $[\beta + \alpha(E - E_0)]$:

$$f(E) = h \left\{ 1 + M_V \left[\frac{E - E_0}{\beta + \alpha(E - E_0)} \right]^2 \right\}^{-1} \times \exp \left\{ -(1 - M_V) \ln 2 \left[\frac{E - E_0}{\beta + \alpha(E - E_0)} \right]^2 \right\} \quad (6)$$

$$f(E) = h M_V \left\{ 1 + \left[\frac{E - E_0}{\beta + \alpha(E - E_0)} \right]^2 \right\}^{-1} + h(1 - M_V) \exp \left\{ -\ln 2 \left[\frac{E - E_0}{\beta + \alpha(E - E_0)} \right]^2 \right\} \quad (7)$$

Besides E_0 and β , the peak height h , the asymmetry index α , and the Lorentzian–Gaussian mixing ratio M_V (L–G mixing) have to be specified.

The advantages of the application of the product-type and sum-type peak-shape models are the availability of analytical presentations of the partial derivatives of $f(E)$ with respect to the parameters, which are needed in the Marquardt–Levenberg algorithm⁶ to establish the Jacobi matrix, the correspondence of experimental $FWHM$ and the analytical value of 2β . Finally, a faster convergence of the iterative process was observed frequently.

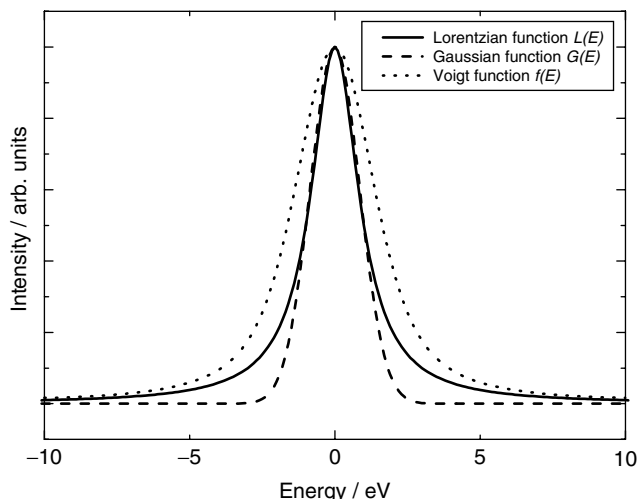


Figure 1. Comparison of a Gaussian and a Lorentzian function with $FWHM = 2$ eV with the result of the convolution of both, the Voigt profile $f(E)$ (Eqn (8), peak height normalized). Note that a Voigt function with $FWHM = 2$ eV lies between the Gaussian and Lorentzian functions with the same $FWHM$.

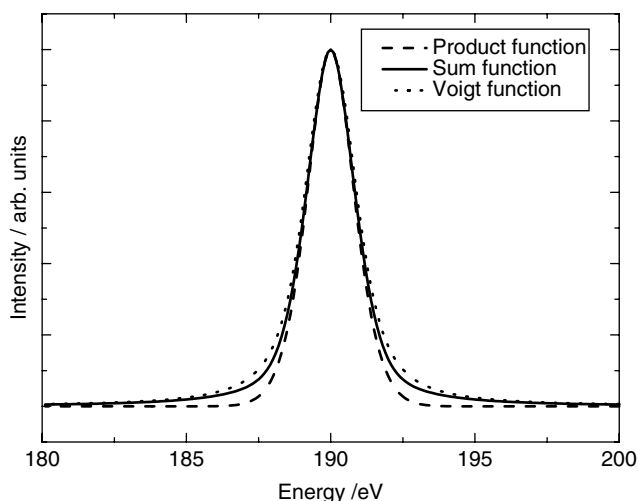


Figure 2. Comparison of symmetric product (Eqn (6), $M_V = 0.5$), sum (Eqn (7), $M_V = 0.5$) and Voigt function (Eqn (8), $GP-FWHM = 1.3$ eV, $LP-FWHM = 1.3$ eV) with $FWHM = 2$ eV, energy position $E_0 = 190$ eV.

In comparison to the sum and product function, a better description of the XPS peaks may be obtained by convolution of independent Gaussian and Lorentzian (or Doniach–Sunjic type) contributions. This convolution giving the so-called Voigt profile (Fig. 2) is defined as follows:

$$f(E) = hf(L * G) = h \int_{-\infty}^{+\infty} L(E')G(E - E')dE' \quad (8)$$

In contrast to the product and sum function, the Voigt function contains independent values for the $FWHM$ s of the Lorentzian and the Gaussian functions ($LP-FWHM$ and $GP-FWHM$). Otherwise, the generation of a Voigt profile is more time consuming. Application of this peak-shape model is highly recommended if the resolution is sufficient to derive physically meaningful peak-shape parameters. This profile

function and the corresponding derivations with respect to the parameters have to be calculated numerically, giving a more time-consuming chi-square minimization process.

Modelling the background

The choice of an adequate model of the spectral background depends on the properties of the sample.

The Shirley background $S(E)$ assumes a constant energy-loss function (Shirley step function).¹³ It has in many cases turned out to be a successful approximation for the inelastic background of core-level peaks.

The Tougaard background $T(E)$ ^{14,15} was originally developed for transition metals, and includes a model shape for the energy-loss function based on a two-parameter universal cross section (available for most metals, their oxides and alloys). The introduction of a third parameter¹⁶ allows the application of the Tougaard background also for polymers, semiconductors and free-electron-like solids. The registration of a large energy window towards lower kinetic energies or larger energy losses is necessary for adopting this background model.

A polynomial of low order has also often been used to model the secondary-electron background or the tails of nearby peaks reasonably well.

A general approach for the characterization of the background in core-level photoelectron spectra⁴ takes into account all of these contributions, weighted appropriately by the background shape parameters $a - f$:

$$B(E) = a + bE + cE^2 + dE^3 + eS(E) + fT(E) \quad (9)$$

The background shape parameters may be varied completely freely or fixed at certain values. An iterative calculation of the background by including suitable parameters $a - f$ in the fit procedure is recommended, independent of the specimen properties.

GENERATION OF SYNTHETIC TEST SPECTRA

In order to demonstrate the validity of different model peak shapes, four test spectra (two without and two with normally distributed noise) were generated independently using MICROCAL ORIGIN. Referring to the work of Seah and Brown,¹⁷ two C 1s spectra that may be found in practice were simulated.¹⁰ The two materials chosen were

PVC: polyvinyl chloride and
PMMA: polymethyl methacrylate.

All test spectra were generated using the convolution routine of MICROCAL ORIGIN with a $LP-FWHM$ and a $GP-FWHM$ of 0.6 eV. The step width was 0.05 eV. The test spectra were symmetric functions ($\alpha = 0$ in the Doniach–Sunjic line shape). These spectra were added to a background function $B(i)$ consisting of a constant and a Shirley background

$$B(i) = 500 + 0.001 \sum_{j=1}^i M(j) \quad (10)$$

with the test spectrum $M(i)$ and the channel number $i = 1$ on the high-energy side. The corresponding parameters are shown in Table 2.

Table 2. Parameters of the generated test spectra

Material	Parameter	Peak number			
		1	2	3	4
PVC	Height/counts	10 000	10 000	–	–
	GL-FWHM/eV	0.600	0.600	–	–
	Position/eV	287.00	285.90	–	–
	LP-FWHM/eV	0.600	0.600	–	–
	Peak area/counts-eV	13 274	13 274	–	–
	Rel. peak area/%	50.0	50.0	–	–
PMMA	Height/Counts	3360	4160	4160	8320
	GL-FWHM/eV	0.600	0.600	0.600	0.600
	Position/eV	289.00	286.80	285.70	285.00
	LP-FWHM/eV	0.600	0.600	0.600	0.600
	Peak area/counts-eV	4460	5522	5522	11 044
	Rel. peak area/%	16.80	20.80	20.80	41.60
	Background	$B(i) = 500 + 0.001 \sum_{j=1}^i M(j)$			

In order to create more realistic test spectra, the test functions PVC and PMMA were also superimposed with normally distributed noise¹⁸ and labelled as PVCs and PMMAs.

RECORDING A Cu 3p SPECTRUM

As an alternative to synthetic test spectra for testing the model functions, a Cu 3p spectrum was recorded with a VG ESCALAB 220 iXL spectrometer equipped with a 220 analyser (double-focussing 180° spherical sector analyser, 150 mm radius) and a set of six channel electron multipliers. The instrument was operated in the CAE mode (constant pass energy) at pass energy of 10 eV and the magnetic lens mode 'Large Area XL'. The step width was 0.1 eV. The X-ray source was an Al anode operated at 10 kV and 20 mA followed by an X-ray monochromator; the number of scans was 3 and the dwell time was 300 ms. The base pressure during the experiment was 5×10^{-10} mbar.

The sample was a metallic foil of size 12×12 mm². To remove contamination, the sample was sputtered using 5 keV argon ions. After sputtering, the C 1s peak in the survey spectrum was below the noise level.

FIT OF SPECTRA

The rate of convergence and the results of iterative chi-square minimization depend sensitively on the starting parameters. Thus, we have started the fit procedure with initial values at least 20% from the ideal values for the peak height. The peak energies were shifted by 0.5 eV. The FWHM was set to 1.0 eV and the L–G mixing to 0.7 using the product or sum model function. In case of Voigt-profile modelling, the starting values of LP-FWHM and GP-FWHM were 0.8 eV. All asymmetry parameters were set to zero and kept fixed. No coupling of parameters was allowed. The free background parameters (test spectra: constant *a* and Shirley parameter *e* were free, parameters *b*, *c*, *d* and *f* were fixed at zero; Cu 3p: only the Tougaard parameter *f* was fixed at zero) were

determined together with the parameters of the model peaks in the fit (Eqn (9)). The correct number of single peaks was preset. For the analysis of the test spectra, only 350 points both to the left and the right of the maximum were used (number of points of the original test spectra was >1000) because the convolution routine of the software MICROCAL ORIGIN made significant errors around the starting and ending regions of the generated spectra.

In UNIFIT 2006,⁵ the reduced chi-square⁷ is calculated to provide the quantity that measures the error of the fit or the deviation of the original data and the fit function. The reduced chi-square is minimized during the iteration procedure. The expectation value of the reduced chi-square should decrease approaching 1 in case of a good fit to spectra with random noise.

However, the PVC and PMMA test spectra were analysed as synthesized, which means that no noise-like contributions were added. Therefore, in case of ideal matching, the error of the fit should be mostly of numerical origin and should actually approach zero. The *Abbe* criterion⁷ provides information on the appearance of correlation of adjacent residuals and thus on possible shortcomings of the fit. The expectation value of the *Abbe* criterion is 1 in case of a good fit with statistically uncorrelated residuals if the residuals are determined only by random noise of the data. The *Abbe* criterion should approach zero for strong correlations among adjacent residuals and would indicate a poor fit. Anti-correlation of the adjacent residuals, as might be anticipated for mostly numerical errors, is indicated by *Abbe* values exceeding 1. This should be considered during the discussion of the following results.

Because the sum function (Eqn (7)) is not available in the standard version of the software UNIFIT, the program code was modified to generate the sum model functions.

Fit of the PVC spectrum

The test spectrum PVC was synthesized from two well-separated single lines, which may be clearly distinguished owing to the valley between the maxima.

Table 3. Fit parameters from the analysis of the test spectrum PVC using the convolution, product and sum of Lorentzian and Gaussian functions

Parameter	Test spectrum PVC					
	Convolution (Eqn (8))		Product (Eqn (6))		Sum (Eqn (7))	
	Peak 1	Peak 2	Peak 1	Peak 2	Peak 1	Peak 2
Height/counts	10 000	10 000	9868	10 411	10 080	10 149
L-G mixing	–	–	0.862	1.000	0.590	0.582
GP-FWHM/eV	0.600	0.600	–	–	–	–
Position/eV	287.00	285.90	286.98	285.89	287.01	285.91
FWHM/eV	–	–	0.99	0.89	0.97	0.99
LP-FWHM/eV	0.600	0.600	–	–	–	–
Peak area/counts·eV	13 273	13 273	11 729	14 349	13 122	13 470
Rel. peak area/%.	50.00	50.00	44.98	55.02	49.35	50.65
Constant background		501		500		498
Shirley background		0.001		0.001		0.001
χ^{2*}		$<10^{-3}$		1.133		0.066
Abbe criterion		0.977		0.051		0.074

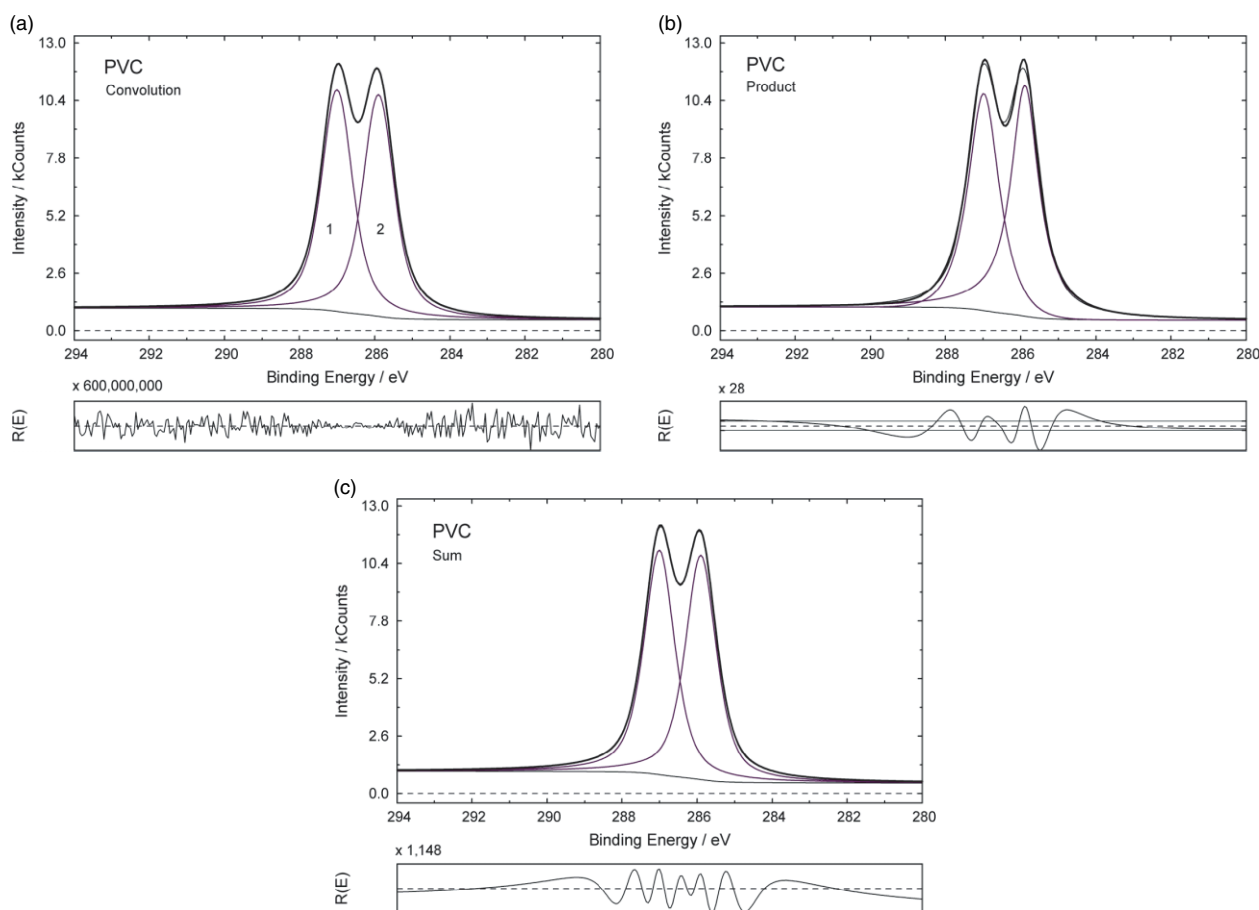


Figure 3. Fit of the test spectrum PVC using the convolution (a), the product (b) and the sum (c) of Lorentzian and Gaussian functions. Notice the different scaling factors of the residual plots. This figure is available in colour online at www.interscience.wiley.com/journal/sia.

The optimized parameters using the Voigt profile (Eqn (8)) represented in Table 3 reproduce the ideal ones, as demonstrated by comparison with Table 2 (see also Fig. 3). A very small reduced chi-square of $<10^{-3}$ and a value of the *Abbe* criterion close to the expected value of 1 indicate successful modelling with the optimized parameters. Only

the constant parameter for the background and the peak areas show very small deviations from the selected parameters for the test spectrum (0.2% and $<0.01\%$). The fit converged very quickly to the global minimum (only 22 iteration cycles). The normalized residual $R(i)$ shows a statistical behaviour and the remaining deviations indicate numerical effects.

The fit using the product function (Eqn (6)) gives the worst result. The product model function may not describe the test spectrum satisfactorily. The systematic deviations become clearly evident in the presentation of the residual. In particular, the estimation of the relative peak area of each peak has an error of more than 10% (Tables 3 and 7). The values $\chi^{2*} > 1.13$ and $Abbe = 0.051$ are far from the ideal value (Table 3 and Fig. 3(b)). Only the energy positions may be estimated with an accuracy of better than 0.02 eV. The calculated values for the L–G mixing of $M_V = 1$ and 0.862 are surprising because the contributions of the Gaussian and Lorentzian functions creating the test spectrum PVC were the same.

The peak fit using the sum function (Eqn (7)) gives definitely more accurate results (Table 3 and Fig. 3(c)). The modelling of the test spectrum is satisfactory over a wide range. The line positions are estimated correctly and the accuracy of the relative peak areas is better than 2%. Also, the calculated mixing ratios of the Lorentzian and Gaussian functions of 0.582 and 0.590 reproduce better the true mixing ratio of the test spectrum. Smaller differences between the test spectrum and the model function are illustrated by the residual function (Fig. 3(c)); the $Abbe$ criterion is 0.074 and the χ^{2*} is 0.066.

Fit of the PVCs spectrum

The analysis of the more realistic test spectrum with normally distributed noise gives small deviations from the true values, independent of the applied model function.

The application of the convolution function (Eqn (8)) delivers excellent results for PVCs also. All deviations of the optimized parameters are caused by statistical noise (Table 4 and Fig. 4(a)). The maximum relative errors of peak height, peak area and relative peak area are less than 1%. The peak positions were estimated correctly without deviations (Table 7). The fit quantities are close to the ideal values.

The product–function fit (Eqn (6)) of the PVCs did not give satisfactory results. Also, the correct ratio of peak heights (50%/50%) was not found. The maximum relative error for

the peak area was >7% (Table 7). The residual function shows systematic errors and the fit quantities are far from the ideal values (Table 4 and Fig. 4(b)).

The analysis of the PVCs-test spectrum with the sum model (Eqn (7)) produces similarly good results. The relative peak area may be found with an accuracy of 1%. The maximum relative error of the peak area is about 3% (Table 7). The residual function shows a nearly statistically distributed behaviour, and the reduced chi-square is close to the expected value of 1 (Table 4 and Fig. 4(c)).

Fit of the PMMA spectrum

In contrast to the double-peak PVC test spectrum, the corresponding PMMA spectrum was composed of four peaks. Two of the peaks in PMMA were very close together and could not be resolved by eye (Fig. 5).

Even this more complex test spectrum could be modelled perfectly using the Voigt profile (Eqn (8), Table 5 and Fig. 5(a)). Again, a χ^{2*} of $<10^{-3}$ and an $Abbe$ criterion of nearly unity were obtained. The optimized fit parameters provided in Table 5 show perfect agreement with the parameters of the test spectrum (Table 2). This result also represents the improved convolution procedure of the program UNIFIT 2006.⁵

Analysis with the product function (Eqn (6), Table 5 and Fig. 5(b)) resulted in large deviations (up to 30%) from the true values. Only the well-separated peaks at 289.0 eV and 286.8 eV were fitted satisfactorily. The peak shapes for the close peaks at 285.7 eV and 285.0 eV could not be described accurately. Large errors of the peak position (of up to 0.23 eV) and of the peak height (of more than 28%) (Table 7) were found.

The results with the sum function (Eqn (7)) were similar to the results using the product function (Table 5 and Fig. 5(c)). The sum function also modelled poorly the close peaks at 285.7 eV and 285.0 eV of the PMMA-test spectrum. The peak height for the third peak at 285.7 eV was obtained very low, giving in turn the second peak at 286.8 eV about 38% too large. Only the first peak was modelled satisfactorily.

Table 4. Fit parameters from the analysis of the test spectrum PVCs using the convolution, product and sum of Lorentzian and Gaussian functions

Parameter	Test spectrum PVCs					
	Convolution (Eqn (8))		Product (Eqn (6))		Sum (Eqn (7))	
	Peak 1	Peak 2	Peak 1	Peak 2	Peak 1	Peak 2
Height/counts	9985	10 081	9861	10 380	10 049	10 247
L-G mixing	–	–	0.860	1.000	0.574	0.593
GP-FWHM/eV	0.606	0.595	–	–	–	–
Position/eV	287.00	285.90	286.98	285.89	287.01	285.91
FWHM/eV	–	–	0.990	0.895	0.970	0.983
LP-FWHM/eV	0.594	0.606	–	–	–	–
Peak area/counts·eV	13 226	13 405	11 730	14 317	12 994	13 681
Rel. peak area/%	49.66	50.34	45.03	54.97	49.02	50.98
Constant background		499		499		496
Shirley background		0.001		0.001		0.001
χ^{2*}		1.089		2.200		1.143
$Abbe$ criterion		0.989		0.279		0.865

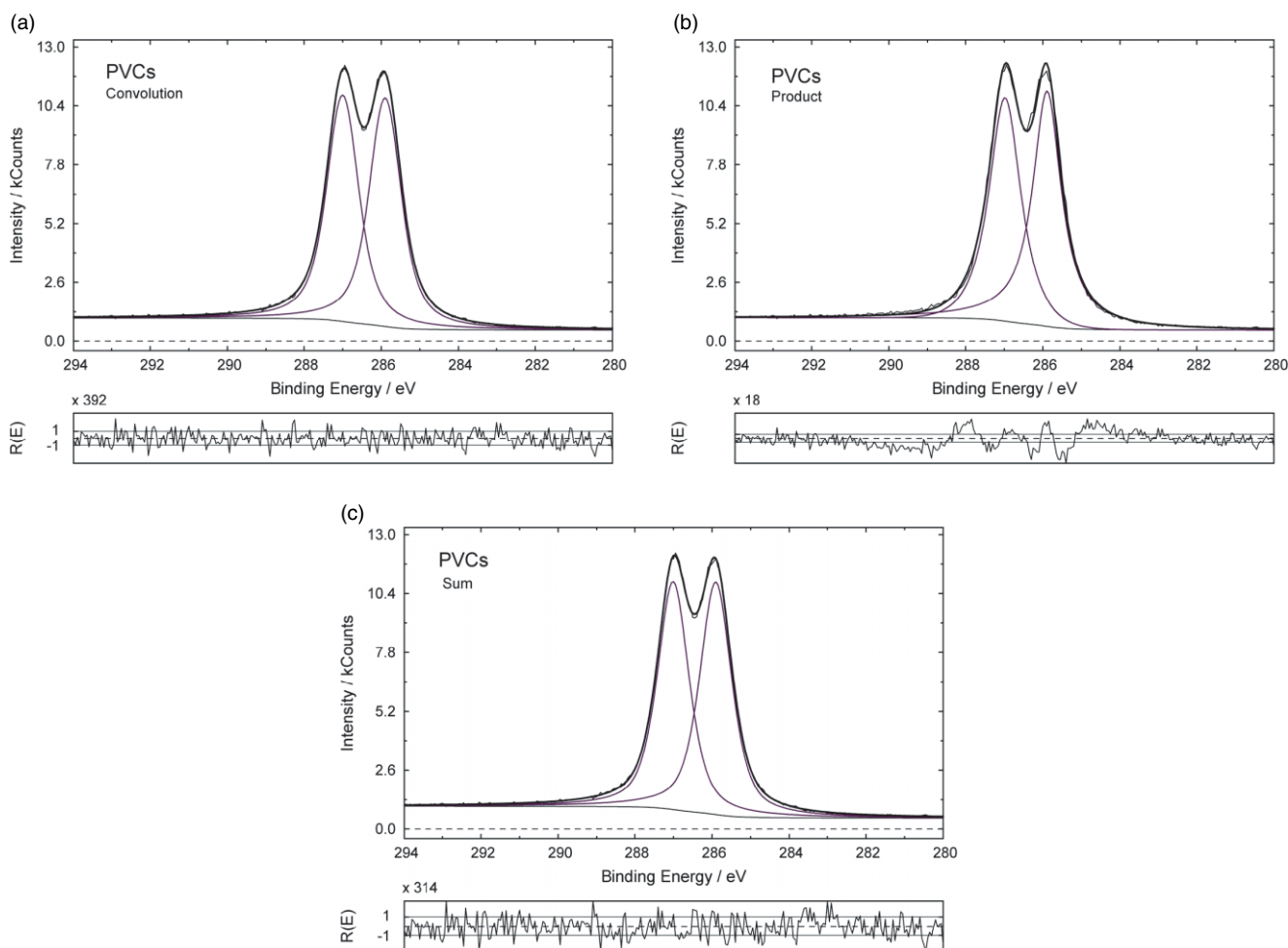


Figure 4. Fits to the test spectrum PVCs using the convolution (a), the product (b) and the sum (c) of Lorentzian and Gaussian functions. Notice the different scaling factors of the residuum plots. This figure is available in colour online at www.interscience.wiley.com/journal/sia.

Table 5. Fit parameters from the analysis of the test spectrum PMMA using the convolution, product and sum of Lorentzian and Gaussian functions

Parameter	Test spectrum PMMA											
	Convolution (Eqn (8))				Product (Eqn (6))				Sum (Eqn (7))			
	Peak 1	Peak 2	Peak 3	Peak 4	Peak 1	Peak 2	Peak 3	Peak 4	Peak 1	Peak 2	Peak 3	Peak 4
Height/counts	3360	4160	4160	8320	3575	4370	5334	6253	3389	4528	3649	9001
L-G mixing	-	-	-	-	0.963	0.737	0.000	1.000	0.611	0.605	0.047	0.639
GP-	0.600	0.600	0.600	0.600	-	-	-	-	-	-	-	-
FWHM/eV												
Position/eV	289.00	286.80	285.70	285.00	288.99	286.81	285.47	284.93	289.00	286.78	285.72	285.01
FWHM/eV	-	-	-	-	0.964	0.996	1.241	0.982	0.981	1.015	0.870	1.000
LP-FWHM/eV	0.600	0.600	0.600	0.600	-	-	-	-	-	-	-	-
Peak area/counts-eV	4458	5520	5520	11 040	4559	4913	7046	9472	4458	6158	3449	12 206
Rel. peak area/%.	16.80	20.80	20.80	41.60	17.54	18.90	27.11	36.45	16.97	23.44	13.13	46.46
Constant background		501				510				500		
Shirley background		0.001				0.001				0.001		
χ^2 *		<10 ⁻³				0.210				0.058		
Abbe criterion		1.186				0.063				0.087		

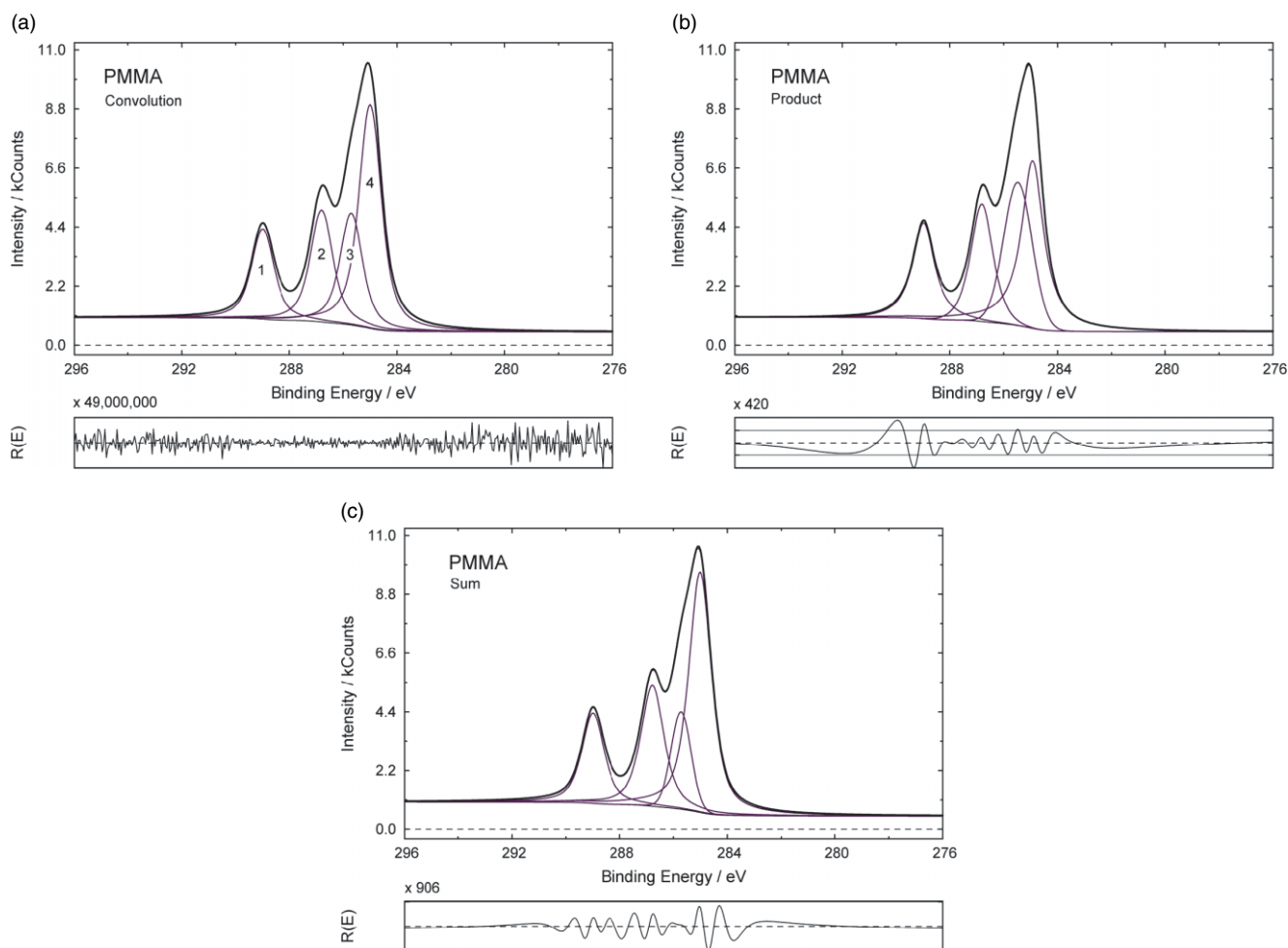


Figure 5. Fits to the test spectrum PMMA using the convolution (a), the product (b) and the sum (c) of Lorentzian and Gaussian functions. Notice the different scaling factors of the residuum plots. This figure is available in colour online at www.interscience.wiley.com/journal/sia.

Table 6. Fit parameters from the analysis of the test spectrum PMMAs using the convolution, product and sum of Lorentzian and Gaussian functions

Parameter	Test spectrum PMMAs											
	Convolution (Eqn (8))				Product (Eqn (6))				Sum (Eqn (7))			
	Peak 1	Peak 2	Peak 3	Peak 4	Peak 1	Peak 2	Peak 3	Peak 4	Peak 1	Peak 2	Peak 3	Peak 4
Height/counts	3377	4169	4038	8662	3572	4412	5234	7058	3410	4449	4817	7.086
L-G mixing	–	–	–	–	0.960	0.677	0.000	1.000	0.628	0.658	0.000	0.808
GP-FWHM/eV	0.587	0.652	0.545	0.610	–	–	–	–	–	–	–	–
Position/eV	289.00	286.80	285.73	285.01	288.98	286.80	285.52	284.92	289.00	286.81	285.56	284.94
FWHM/eV	–	–	–	–	0.978	0.995	1.167	0.926	0.987	0.962	1.186	0.966
LP-FWHM/eV	0.633	0.527	0.598	0.593	–	–	–	–	–	–	–	–
Peak area/ counts·eV	4583	5357	5149	11 505	4672	4854	6499	10 092	4594	5906	6084	9929
Rel. peak area/%.	17.23	20.15	19.36	43.26	17.89	18.58	24.89	38.64	17.33	22.28	22.95	37.45
Constant background		499				506				498		
Shirley background		0.001				0.001				0.001		
χ^2 *		1.103				1.354				1.147		
Abbe Kriterium		0.979				0.658				0.851		

The estimated values of the fit quantities χ^{2*} and *Abbe* criterion (Table 5) are definitely better, but the maximum of the relative uncertainty of the relative peak area (36.9%) is higher than that for the product model. Nevertheless, the maximum error of the peak position is only 0.02 eV (Table 7).

Fit of the PMMAs spectrum

The PMMAs-test spectrum best represents a realistic measurement. The combination of two separate peaks and two very close lines with superimposed normally distributed noise simulates a real spectrum very realistically.

The fit using the Voigt profile (Eqn (8)) gives very good results for all four peaks. In particular, the positions of the two unseparated peaks at 285.70 eV and 285.00 eV were found with uncertainties of <0.03 eV. The maximum uncertainties of the peak height and peak area were about 4 and 7% respectively (Tables 6 and 7, Fig. 6(a)). χ^{2*} and the *Abbe* criteria were 1.103 and 0.979.

A poor fit was obtained with the product model function (Eqn (6)). The results and errors of the fit of the PMMAs-test spectrum with respect to the fit of the PMMA-test spectrum were similar. In both cases the same areas expected for the peaks at 286.8 and 285.7 eV were not found (area fit results: 1 : 1.43 and 1 : 1.34). Only the design parameters for the peak heights and peak positions of the first and second peak were estimated satisfactorily with an error better than 5% and 0.02 eV respectively. The maximum relative error of all

Table 7. Maximum uncertainty of fit parameters peak height Δh , peak position ΔE_0 , peak area ΔI and relative peak area ΔI_{rel} for fits of the test spectra PVC, PVCs, PMMA and PMMAs using the convolution, product and sum model functions

Test spectrum	Model function	Maximum uncertainty of fit parameters			
		$\Delta h/\%$	$\Delta E_0/\text{eV}$	$\Delta I/\%$	$\Delta I_{rel}/\%$
PVC	Convolution	0.00	0.00	0.01	0.00
	Product	4.11	0.02	11.64	10.04
	Sum	1.49	0.01	1.48	1.30
PVCs	Convolution	0.81	0.00	0.99	0.68
	Product	3.8	0.02	7.86	9.94
	Sum	2.47	0.01	3.07	1.95
PMMA	Convolution	0.00	0.00	0.04	0.00
	Product	28.22	0.23	27.60	30.34
	Sum	12.28	0.02	37.54	36.87
PMMAs	Convolution	4.11	0.03	6.75	3.99
	Product	25.82	0.18	17.70	19.66
	Sum	14.83	0.14	10.18	10.34

estimated relative peak areas was about 20% (Table 7). The values of χ^{2*} and the *Abbe* criterion (1.354 and 0.658) illustrate the poor result (Table 6 and Fig. 6(b)).

The results of the peak fit of the PMMAs spectrum with the sum model were better than the PMMA spectrum

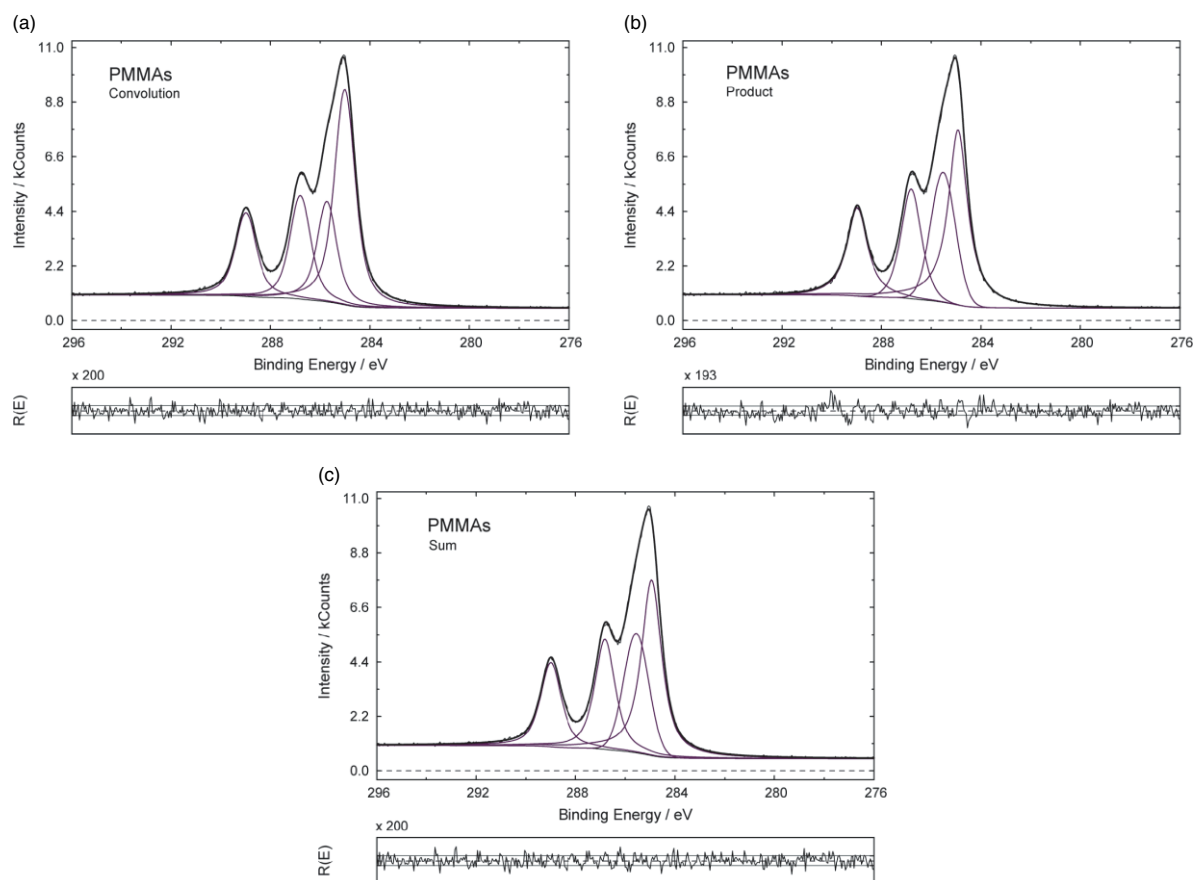


Figure 6. Fits to the test spectrum PMMAs using the convolution (a), the product (b) and the sum (c) of Lorentzian and Gaussian functions. Notice the different scaling factors of the residuum plots. This figure is available in colour online at www.interscience.wiley.com/journal/sia.

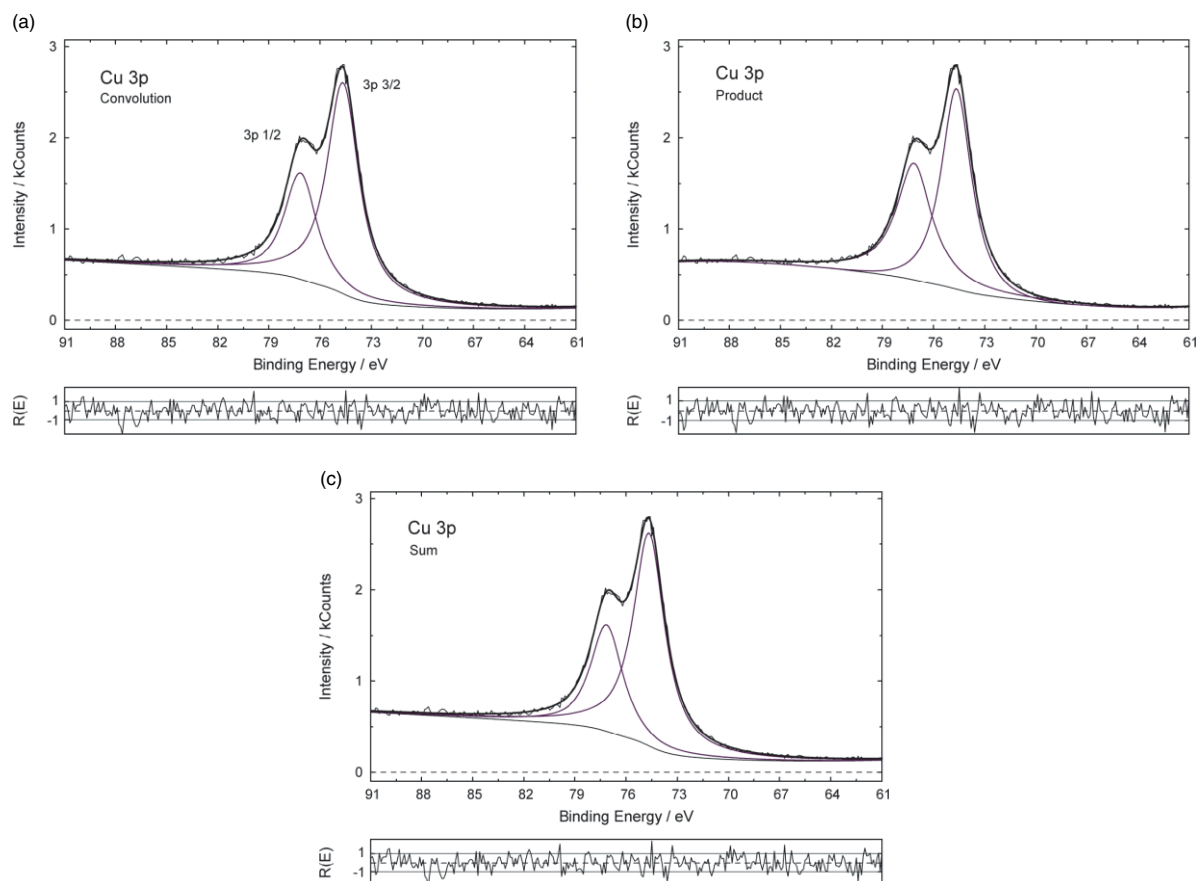


Figure 7. Fits to the Cu 3p spectrum using the convolution (a), the product (b) and the sum (c) of Lorentzian and Gaussian functions. This figure is available in colour online at www.interscience.wiley.com/journal/sia.

(Eqn (7)). The spectrum with statistical noise was easier to fit and to obtain the correct fit parameters. χ^2 and the *Abbe* criterion were 1.147 and 0.851 (Table 6) and the normalized residual function shows a statistical behaviour (Fig. 6(c)). All fit parameters were closer to their expected values than found with the product model. The relative uncertainties of all parameters were less than 15% (Table 7).

Fit of a Cu 3p Spectrum

We wished to test the three models (Eqns (6)–(8)) using a real spectrum, which ideally should have the following desirable spectral features:

1. Two overlapping peaks with a clear separation.
2. A well-known intensity ratio of the components.
3. Nearly equal contributions of Gaussian and Lorentzian functions describing each peak shape.

The chosen Cu 3p doublet is a suitable real test peak for the first two points. Unfortunately, the peak is more like a Lorentzian than a Gaussian for our measurement conditions.

Figure 7 shows the Cu 3p spectrum fitted with the convolution model function (Eqn (8), Fig. 7(a)), with product model function (Eqn (6), Fig. 7(b)) and with the sum model function (Eqn (7), Fig. 7(c)). Table 8 lists values of all fit parameters. The binding energies and the energy difference of 2.47 eV are exactly the same for all three methods, but the ratios of the peak areas of the $3p_{3/2}$ and $3p_{1/2}$ peaks are different. The standard ratio coming from atomic theory is 2:1. For the

convolution and the sum models, ratios of 2.04:1 and 2.06:1 respectively were found close to the expected 2:1 ratio. The product model gave an unacceptable doublet ratio of 1.23:1.

The point of interest here is the very good statistics of the residual function, and the similar values of the reduced chi-square and *Abbe* criterion found with all three methods. These fits gave satisfactory peak fits but did not give any information on the relative validity of the model functions.

The above results are in contrast to those of a Cu 3p fit using different model functions by Gong.¹⁹ He found smaller errors using the product function than with the sum function. However, Gong subtracted a Shirley background before the peak fit, and the residual distribution for evaluating the peak-shape analysis was not shown.

SUMMARY

The choice of an adequate model function to fit XPS spectra is necessary so that the fit parameters can be meaningfully correlated with the chemical species. Three models are commonly used: product, sum and convolution of Gaussian and Lorentzian functions. In tests of synthetic peak structures using convolved Gaussian and Lorentzian functions as well as one measured Cu 3p peak, the sum function was found to be superior to the product function. The analysis using convolved Gaussian and Lorentzian functions, of course, worked best.

Peak fits using the three different model functions show strong differences in the resulting fit parameters.

Table 8. Fit parameters for the analysis of the Cu 3p spectrum using the convolution, product and sum model functions

Parameter	Cu 3p					
	Convolution (Eqn (8))		Product (Eqn (6))		Sum (Eqn (7))	
	3p _{1/2}	3p _{3/2}	3p _{1/2}	3p _{3/2}	3p _{1/2}	3p _{3/2}
Height/counts	1294	2568	1419	2439	1297	2592
L-G mixing	–	–	1.000	0.899	0.812	0.927
GP-FWHM/eV	0.866	0.646	–	–	–	–
Position/eV	77.5	75.1	77.5	75.1	77.5	75.1
FWHM/eV	–	–	2.475	2.127	2.226	2.218
LP-FWHM/eV	1.86	2.03	–	–	–	–
Peak area/counts·eV	4142	8454	5227	6440	4087	8424
Rel. peak area/%.	32.89	67.11	44.80	55.20	32.67	67.33
Peak area ratio		2.04		1.23		2.06
<i>a</i>		150.54		165.80		149.64
<i>b</i>		–0.565		–0.861		–0.563
Background <i>c</i>		0.0069		0.0220		0.0062
<i>d</i>		-9.8×10^{-6}		-4.8×10^{-5}		-8.1×10^{-6}
<i>e</i>		0.00317		0.0011		0.00326
χ^2 *		0.701		0.697		0.706
Abbe criterion		0.815		0.816		0.807

As expected, fit parameters from the convolved Gaussian and Lorentzian function (Voigt model, Eqn (8)) gave the best results. The derived fit parameters for the test spectra PVC and PMMA agreed with the design values and illustrated the improved convolution subroutine of the program UNIFIT 2006.⁵ Also, the test spectra PVCs and PMMAs, in which realistic levels of noise were added, were fitted successfully with the Voigt profile. The relative errors of the derived parameters of all fitted test spectra were less than 7%. Also, the fitting of the real Cu 3p spectrum gave the correct peak area ratio of the doublet lines.

The worst result of the peak form analysis of the test spectra was achieved with the product model (Eqn (6)). Large relative deviations of the estimated fit parameters with respect to the design values for almost all test spectra illustrate that the unsatisfactory fit gives errors of line position up to 0.23 eV and relative deviations of the peak height up to 28%. A wrong doublet ratio of 1.23:1 for the real Cu 3p spectrum confirms the results of the test spectra.

In accord with the close similarity between the sum and the Voigt profile (Fig. 2), the sum model (Eqn (7)) gave satisfactory results. For only one spectrum (PMMA) was the error higher than for the product function. In all other cases, including the real Cu 3p spectrum, the fit results were significantly better with the sum function.

This investigation has shown that fits of photoelectron peaks with nearly the same Lorentzian and Gaussian amounts using the three different model functions give large differences of the estimated fit parameters. However, for nearly pure Lorentzian or Gaussian peak shapes of the spectral components, the fit results for the three models cannot be distinguished.

Sherwood's recommendation of the product function for the modelling of photoelectron spectra² could not be confirmed. Our results may stimulate further analysis of real

photoelectron spectra comparing the Voigt, the sum and the product model functions for fitting XPS spectra.

Acknowledgements

The authors are indebted to the referees for many helpful comments and corrections.

REFERENCES

1. Doniach S, Sunjic M. *J. Phys. C* 1970; **3**: 285.
2. Sherwood PMA. In *Practical Surface Analysis*, Briggs D, Seah MP (eds). John Wiley: Chichester, 1984; 459.
3. Grant JT. In *Surface Analysis by Auger and X-Ray Photoelectron Spectroscopy*, Briggs D, Grant JT (eds). IM Publications: Chichester, 2003; 861.
4. Hesse R, Chassé T, Szargan R. *Fresenius J. Anal. Chem.* 2003; **365**: 48, www.uni-leipzig.de/~unifit [2006].
5. www.uni-leipzig.de/~unifit [2006].
6. Marquardt DW. *J. Soc. Ind. Appl. Math.* 1963; **11**: 431.
7. Hesse R, Chassé T, Streubel P, Szargan R. *Surf. Interface Anal.* 2004; **36**: 1373, www.uni-leipzig.de/~unifit [2006].
8. Ansell RO, Dickinson T, Povey AF, Sherwood PMA. *J. Electroanal. Chem.* 1979; **98**: 79.
9. Sherwood PMA. In *Practical Surface Analysis* (2nd edn), vol. 1, Briggs D, Seah MP (eds). John Wiley: Chichester, 1990; 573.
10. Beamson G, Briggs D. *High Resolution XPS of Organic Polymers*. John Wiley: Chichester, 1992.
11. *Scienta ESCA300 Users' Manual*. Scienta: Uppsala, 1992.
12. Fairley N. In *Surface Analysis by Auger and X-Ray Photoelectron Spectroscopy*, Briggs D, Grant JT (eds). IM Publications: Chichester, 2003; 401.
13. Shirley DA. *Phys. Rev., B* 1972; **5**: 4709.
14. Tougaard S, Jørgensen B. *Surf. Interface Anal.* 1985; **7**: 17.
15. Tougaard S, Braun W, Holub-Krappe E, Saalfeeld H. *Surf. Interface Anal.* 1988; **13**: 225.
16. Tougaard S. *Surf. Interface Anal.* 1997; **25**: 137.
17. Seah MP, Brown MT. *J. Electron Spectrosc. Relat. Phenom.* 1998; **95**: 71.
18. Box GEP, Muller ME. *Ann. Math. Stat.* 1958; **29**: 610.
19. Gong Y. *Trace Microprobe Techn.* 1997; **15**(4): 399.